Cytoplasmic Dynein Is Required for Distinct Aspects of MTOC Positioning, Including Centrosome Separation, in the One Cell Stage *Caenorhabditis elegans* Embryo

Pierre Gönczy, Silke Pichler, Matthew Kirkham, and Anthony A. Hyman

*European Molecular Biology Laboratory, Heidelberg, D-69117 Germany; and ‡Max-Planck Institute for Cell Biology and Genetics, Dresden, D-01307 Germany

Abstract. We have investigated the role of cytoplasmic dynein in microtubule organizing center (MTOC) positioning using RNA-mediated interference (RNAi) in *Caenorhabditis elegans* to deplete the product of the dynein heavy chain gene *dhc-1*. Analysis with time-lapse differential interference contrast microscopy and indirect immunofluorescence revealed that pronuclear migration and centrosome separation failed in one cell stage *dhc-1 (RNAi)* embryos. These phenotypes were also observed when the dynactin components p50/dynamitin or $p150^{Glued}$ were depleted with RNAi. Moreover, in 15% of *dhc-1 (RNAi)* embryos, centrosomes failed to remain in proximity of the male pronucleus. When dynein heavy chain function was diminished only partially with RNAi, centrosome separation took place, but orientation of the mitotic spindle was defective. Therefore, cytoplasmic dynein is required for multiple aspects of MTOC positioning in the one cell stage *C. elegans* embryo. In conjunction with our observation of cytoplasmic dynein distribution at the periphery of nuclei, these results lead us to propose a mechanism in which cytoplasmic dynein anchored on the nucleus drives centrosome separation.

Key words: microtubules • minus end–directed motor • mitosis • RNAi • MTOC positioning

PROPER positioning of microtubule organizing centers (MTOCs)[1] is central to a number of cell division processes. Correct separation of MTOCs is necessary for bipolar spindle formation, whereas accurate positioning of spindle poles during mitosis dictates proper cleavage furrow placement in animal cells. The mechanisms responsible for MTOC positioning are incompletely understood, but they probably involve microtubule-dependent motors that pull or push MTOCs to appropriate cellular locations.

Cytoplasmic dynein, the major minus end–directed microtubule-dependent motor in eukaryotic cells, has been postulated to play a role in several aspects of MTOC positioning (for reviews see Holzbaur and Vallee, 1994; Vallee and Sheetz, 1996; Hirokawa et al., 1998). This multisubunit mechanochemical enzyme is composed of two heavy chains and several intermediate and light intermediate chains. The heavy chains are each ~500 kD in size, and their ATPase activity generates the force that results in translocation along microtubules. Biochemical and genetic data indicate that cytoplasmic dynein requires the presence of the multisubunit complex dynactin for proper function (for reviews see Allan, 1994; Schroer et al., 1996). Cytoplasmic dynein is present throughout the cytoplasm in a punctate manner in most interphase cells, and is enriched at kinetochores during prometaphase, as well as on the spindle during metaphase and anaphase (Pfarr et al., 1990; Steuer et al., 1990; Lin and Collins, 1992; Busson et al., 1998). In polarized MDCK cells, cytoplasmic dynein is enriched in addition at the periphery of nuclei and at discrete cortical sites during metaphase and anaphase (Busson et al., 1998).

The actual role of cytoplasmic dynein in MTOC positioning in complex eukaryotes has not been clearly established. Initial evidence for an involvement came from antibody injection experiments in vertebrate cells (Vaisberg et al., 1993). Injection of function-blocking antibodies against the dynein heavy chain resulted in a failure of centrosome separation. However, in subsequent experiments, injection of mAbs against a dynein light intermediate chain, while perturbing spindle assembly and focusing of

Address correspondence to Pierre Gönczy, European Molecular Biology Laboratory, 1, Meyerhofstrasse, Heidelberg, D-69117 Germany. Tel.: 49-6221-387-337. Fax: 49-6221-387-512. E-mail: gonczy@embl-heidelberg.de

1. *Abbreviations used in this paper:* DIC, differential interference contrast; ds, double-stranded; MTOC, microtubule organizing center; NEB, nuclear envelope breakdown; RNAi, RNA-mediated interference; ss, single-stranded.

spindle poles, did not prevent centrosome separation (Gaglio et al., 1997). A similar outcome was observed when the dynactin complex was inactivated by overexpression of the dynactin component p50/dynamitin (Echeverri et al., 1996). A complication in interpreting these apparently contradictory results is that neither antibody injections nor disruption of dynactin necessarily faithfully reflect the consequences of a loss of cytoplasmic dynein function.

An alternative experimental approach has been the investigation of cytoplasmic dynein function in genetic systems, where loss-of-function phenotypes can be examined. In *Saccharomyces cerevisiae*, null mutations in the genes encoding the dynein heavy chain or a dynactin component result in defective positioning of the spindle pole body at the bud neck during mitosis (Eshel et al., 1993; Li et al., 1993; Clark and Meyer, 1994; Muhua et al., 1994). These mutants undergo normal spindle pole body separation. Moreover, they are viable, demonstrating that cytoplasmic dynein is dispensable in *S. cerevisiae*. In contrast, cytoplasmic dynein is essential in complex eukaryotes such as *Drosophila* and mice since animals homozygous for mutations in the dynein heavy chain gene die during early development (Gepner et al., 1996; Harada et al., 1998). Analysis of weak alleles in *Drosophila* revealed a role for cytoplasmic dynein in spindle orientation during oogenesis, whereas that of homozygous mutant blastocysts in mice confirmed a requirement for localizing the Golgi apparatus that had been suggested by earlier studies (Corthesy-Theulaz et al., 1992; Gepner et al., 1996; Burkhardt et al., 1997; Harada et al., 1998). However, cells bearing strong loss-of-function mutations in the dynein heavy chain die in *Drosophila* and fail to proliferate in culture in mice, thus, hampering analysis of cytoplasmic dynein function in cell division processes (Gepner et al., 1996; Harada et al., 1998). Therefore, the role of cytoplasmic dynein in MTOC positioning in complex eukaryotes remains to be unambiguously determined.

We sought to address this question by abolishing cytoplasmic dynein function in the one cell stage *C. elegans* embryo with RNA-mediated interference (RNAi). In this approach, expression of a given gene in the early embryo is specifically silenced via microinjection of a corresponding fragment of double-stranded (ds) RNA in the gonad of the mother (Fire et al., 1998). Since the targeted germ cells undergo no cell division between the time of injection and fertilization, the one cell stage embryo is the first cell in which a potential requirement for cytoplasmic dynein during mitosis may be uncovered. Importantly, cell division processes and MTOC positioning can be analyzed with great detail in this 50-μm-long cell, both with time-lapse differential interference contrast (DIC) microscopy and indirect immunofluorescence (Nigon et al., 1960; Sulston et al., 1983; Albertson, 1984; Hyman and White, 1987; Gönczy et al., 1999). There are three major forms of centrosome positioning in the one cell stage *C. elegans* embryo. First, centrosomes separate to become positioned on either side of the male pronucleus. Second, centrosomes migrate with the associated male pronucleus, away from the posterior cortex. Third, the centrosome pair rotates to become oriented onto the longitudinal axis, a prerequisite for proper spindle orientation. It has been shown recently using RNAi that the dynactin components $p150^{Glued}$ (known as *dnc-1* in *C. elegans*) and p50/dynamitin (known as *dnc-2*) are required for the latter form of centrosome positioning, and, thus, for correct spindle orientation (Skop and White, 1998). However, no other defects in MTOC positioning were observed in one cell stage embryos, suggesting that cytoplasmic dynein may not be required for centrosome separation in complex eukaryotes.

In this study, we used RNAi to directly examine the role of the force producing dynein heavy chain in MTOC positioning. Our data demonstrate that the dynein heavy chain is required for pronuclear migration and centrosome separation in the one cell stage embryo. We also find that $p150^{Glued}$ and p50/dynamitin are required for these processes, in contrast to what has been reported recently (Skop and White, 1998). In addition, we observe that cytoplasmic dynein is involved in maintaining a tight association between centrosomes and male pronucleus. In conjunction with the presence of cytoplasmic dynein at the periphery of nuclei, these results lead us to propose a mechanism in which cytoplasmic dynein, anchored on the nucleus, drives centrosome separation.

Materials and Methods

Antidynein Heavy Chain Antibodies

A peptide predicted to be unique among *C. elegans* proteins and corresponding to the 19 amino-terminal residues from DHC-1 plus a cysteine (MDSGNESSIIZPPNLKC) was synthesized, conjugated to maleimide-activated keyhole limpet hemocyanin (Pierce Chemical Co.), mixed with titer max adjuvant (Boehringer Ingelheim Ltd.), and injected into rabbits at the European Molecular Biology Laboratory animal house according to standard procedures. The third bleed was affinity-purified against a column of sulfolink coupling gel (Pierce Chemical Co.) coupled to the peptide. Anti–DHC-1 antibodies were eluted with 100 mM glycine, pH 2.5, dialyzed against PBS, and concentrated to 0.8 mg/ml in 50% glycerol.

Worm Protein Extract and Western Blotting

Worms from mixed developmental stages were floated off four 9-cm petri dishes with H_2O, spun for 2 min at 2,000 rpm in a tabletop clinical centrifuge, and resuspended for a wash in 30 ml H_2O. Worms were spun as above, resuspended in 1.5 ml H_2O, transferred to an Eppendorf tube, and spun for 2 min in a microfuge, yielding a pellet of ~100 μl. 200-μl modified 2× loading buffer (M2LB: 100 mM Tris, pH 6.8, 200 mM DTT, 4% SDS, 0.2% bromophenol blue, 20% glycerol, 1 mM PMSF, 10 μg/μl of each leupeptin, pepstatin, and chemostatin) was added to the pellet. The extract was vortexed for 30 s, boiled for 2 min, supplemented with 100 μl M2LB, vortexed for 30 s, boiled for 1 min, and snap-frozen in liquid nitrogen. Cytoplasmic extracts of unfertilized *Xenopus* eggs arrested in metaphase of meiosis II were prepared according to standard procedures (Murray, 1991).

20-μl *C. elegans* extract or 1-μl *Xenopus* extract was loaded per lane on a 6% SDS–acrylamide gel. Proteins were transferred onto nitrocellulose in SDS gel running buffer containing 10% methanol. After blocking, the filter was incubated for 90 min at room temperature with primary antibodies (1:200 rabbit anti–DHC-1 or 1:1,000 mouse anti-*Xenopus* dynein heavy chain, a gift from Sigrid Reinsch, NASA Ames Research Center, Moffet Field, CA). Signal detection was performed with standard enhanced chemiluminescence kit components (Amersham Life Science, Inc.).

Quantitation of Anti–DHC-1 Reactivity in Wild-type and dhc-1 (RNAi) Embryos

dhc-1 (RNAi) embryos gave rise to a fully penetrant phenotype recognizable by staining with antitubulin antibodies (see Results). Therefore, levels of anti–DHC-1 reactivity were analyzed in wild-type and *dhc-1 (RNAi)* embryos 30 h after injection and processed on the same slide to eliminate potential slide-specific differences in staining intensities. Early embryos

(as judged by the DNA stain, <30 nuclei in wild type, and the approximate equivalent in *dhc-1 (RNAi)*) were examined for antitubulin reactivity. Embryos with a strong antitubulin signal were deemed to be properly fixed and stained, and were retained for subsequent analysis of anti–DHC-1 reactivity. Anti–DHC-1 reactivity was imaged with a 4912 Cohu CCD camera set on manual. Mean pixel intensity was determined for each embryo using Adobe Photoshop 4.0, and expressed as a percentage of the average staining intensity of wild-type embryos on each slide. 5–8 of each wild-type and *dhc-1 (RNAi)* embryos were examined per slide.

Generation of Double-stranded RNAs

Double-stranded (ds) RNA corresponding to the dynein heavy chain gene *dhc-1* (T21E12.4) was generated in the following manner. A λZAPII phage containing a 1.3-kb cDNA insert (yk161f11) was obtained from Yuji Kohara (National Institute of Genetics, Mishima, Japan). The insert was PCR-amplified from ~2.4×10^4 phage particles using primers corresponding to vector sequences flanking the insert and that contain consensus sequences for T3 (forward primer) or T7 (reverse primer) RNA polymerases. The PCR product was purified using the QIAquick PCR purification kit (Qiagen). About 0.5 μg was used as a template in 20 μl T3 and T7 RNA polymerase reactions to generate sense and antisense single-stranded (ss) RNAs (RiboMAX™; Promega Corp.). After treatment for 15 min at 37°C with 0.5 U RQ1 DNAse, the RNAs were extracted with phenol/chloroform and resuspended in 20 μl H_2O. An aliquot was run next to RNA standards on a 1% TBE agarose gel to estimate the quality and quantity of RNA generated. Typically, 20–50 μg (1–2.5 μg/μl) of RNA was produced per reaction. To generate dsRNA, equal volumes of sense and antisense ssRNAs were mixed with 1 vol of 3× injection buffer (20 mM KPO_4, pH 7.5, 3 mM potassium citrate, pH 7.5, 2% PEG 6000), incubated 10 min at 68°C and 30 min at 37°C. The resulting dsRNA was aliquoted, snap-frozen in liquid nitrogen, and stored at −70°C.

The same batch of yk161f11 dsRNA was used to quantify all the phenotypic manifestations reported in the text. However, other batches of yk161f11 dsRNA gave identical phenotypes, as did *dhc-1* dsRNAs generated from four other sources: (1) a 1.6-kb cDNA insert in λZAPII from Yuji Kohara, yk166g8; (2) T21E12.4-5, a PCR fragment corresponding to exon 2 and part of exon 3 of *dhc-1*, positions 358–1803 in cosmid T21E12; (3) T21E12.4-M, a PCR fragment corresponding to the end of exon 7 and most of exon 8, positions 6636–7844 in T21E12; and (4) T21E12.4-3, a PCR fragment corresponding to exons 13–15, positions 13420–14854 in T21E12 dsRNAs 2–4 were generated by Alan Coulson at the Sanger Center. dsRNA (2) was used for injections that yielded *dhc-1 (RNAi)* embryos shown in Figs. 6 and 8.

To generate dsRNA corresponding to $p150^{Glued}$ (*dnc-1*) and p50/dynamitin (*dnc-2*), wild-type (N2) genomic DNA was PCR-amplified with primers corresponding to fragments of either gene plus 30 nucleotides for binding of T3 (forward primer) or T7 (reverse primer) RNA polymerases. The following primer pairs were used: (1) dnc-1 (A), covering exons 4, 5, and 6 of *dnc-1*, positions 18537–20065 in cosmid ZK593; (2) dnc-1 (B), covering exons 8, 9, 10, and 11, positions 20843–22155 in cosmid ZK593; and (3) dnc-2, corresponding to all five exons of the *dnc-2* gene, positions 41836–43012 in cosmid Z28H8. Generation of dsRNA was as described above. All primer sequences can be obtained upon request.

Analysis of Embryos by Time-lapse DIC Microscopy and Indirect Immunofluorescence

Wild-type (N2) adult hermaphrodites were injected bilaterally in the gonads according to standard procedures, and placed at 20°C. Animals were dissected 24–30 h after injection and their embryos analyzed by time-lapse DIC microscopy (1 frame every 5 s) or indirect immunofluorescence as previously described (Gönczy et al., 1999).

The following primary antibodies were used: 1:100 or 1:200 rabbit anti–DHC-1, 1:100 rabbit anti–ZYG-9 (Matthews et al., 1998), 1:5,000 rabbit anti–PGL-1 (Kawasaki et al., 1998), and 1:400 mouse antitubulin (clone DM1A; Sigma Chemical Co.). For peptide blocking experiments, slides were preincubated for 15 min with 0.1 mg/ml DHC-1 peptide, and then incubated with anti–DHC-1 antibody in the continued presence of peptide. Secondary antibodies were 1:800 goat anti–mouse Alexa488 (Molecular Probes Inc.) and 1:1,000 donkey anti–rabbit Cy3 (Dianova). Slides were counterstained with Hoechst 33258 (Sigma Chemical Co.) to reveal DNA. Indirect immunofluorescence data were gathered on a confocal microscope (LSM510; Carl Zeiss). All high magnification images are 1.2-μm confocal slices; the stage was refocused slightly between channels in some cases. Images were processed with Adobe Photoshop 4.0.

Velocity Measurements of Yolk Granules

Time-lapse DIC microscopy was performed at 1 frame every 0.5 s to determine the velocity of the fast minus end–directed movements of yolk granules towards the center of asters. In wild type, the focal plane was that of the center of the anterior aster. In *dhc-1 (RNAi)* embryos, the focal plane included the center of both asters, which are together at the very posterior of these embryos (see Results). The analysis was carried out during the ~2 min separating pronuclear envelope breakdown from anaphase in wild-type, when these motility events are most frequent, and the corresponding time interval in *dhc-1 (RNAi)* embryos. The analysis was restricted to motility events that lasted 2 s or more. Average peak velocities were determined using the public domain NIH Image program 1.62b7 (developed at the National Institutes of Health and available at http://rsb.info.nih.gov/nih-image/).

Time-lapse DIC microscopy was performed at 1 frame every 5 s to determine the velocity of the posteriorly directed flows of yolk granules that occur just before pronuclear migration in the cytoplasm posterior of the pseudocleavage furrow (Hird and White, 1993). As noted previously (Hird and White, 1993), these movements are sometimes turbulent, so that calculated velocities should be considered only as best estimates. Average peak velocities were determined as above.

Results

Generation of Antibodies Against the Conventional Cytoplasmic Dynein Heavy Chain DHC-1

We sought to determine the function of conventional cytoplasmic dynein in MTOC positioning in the one cell stage *C. elegans* embryo. There are two cytoplasmic dynein heavy chain genes in the *C. elegans* genome, *dhc-1* (gene T21E12.4; Lye et al., 1995) and *che-3* (gene F18C12.1). We focused our analysis on *dhc-1* because the corresponding protein is more similar to the vertebrate conventional cytoplasmic dynein heavy chain MAP1C (57% amino acid identity along the entire protein as opposed to 30% for CHE-3). Moreover, a putative null allele of *che-3* is viable and has defects restricted to sensory neuron structure and function (Wicks, S., C. de Vries, and R.H.A. Plasterk, personal communication). Accordingly, we did not observe a phenotype in early embryos when *che-3* expression was silenced with RNAi (data not shown).

We began our study by raising polyclonal antibodies against an amino-terminal peptide of DHC-1 (see Materials and Methods). Affinity-purified anti–DHC-1 antibodies recognized two bands on a Western blot of total *C. elegans* proteins: a very high molecular mass species and a species of ~180 kD (Fig. 1 A). The very high molecular mass species most likely corresponds to the dynein heavy chain, which is predicted to be 512 kD in size (Lye et al., 1995). Compatible with this view, this species comigrated with a *Xenopus* protein recognized by anti-*Xenopus* dynein heavy chain antibodies (Fig. 1 A). The lower molecular mass species may correspond to a degradation product of the dynein heavy chain or a distinct cross-reactive species.

We tested whether anti–DHC-1 antibodies specifically recognize dynein heavy chain protein in *C. elegans* embryos in two ways. First, we compared the immunofluorescence staining intensity observed with anti–DHC-1 antibodies in wild type to that seen in embryos in which *dhc-1* gene expression was silenced in a sequence-specific manner using RNAi (hereafter referred to as *dhc-1 (RNAi)*

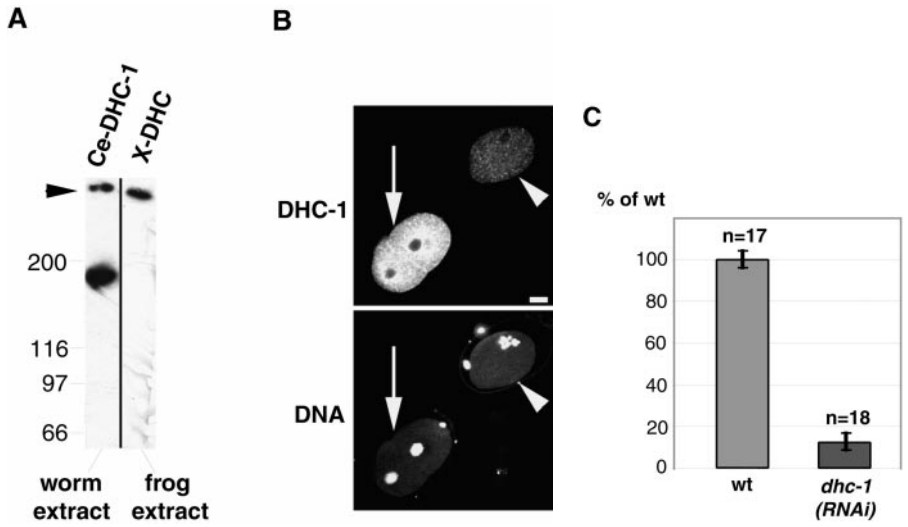

Figure 1. Characterization of anti–DHC-antibodies. (A) Western blot of *C. elegans* (left lane) or *Xenopus* (right lane) extracts probed with antibodies raised against a *C. elegans* DHC-1 peptide (left lane) or a portion of *Xenopus* DHC (right lane). Both antibodies recognize a similarly migrating very high molecular mass species (arrowhead). In addition, the *C. elegans* antibodies recognize a species of ~180 kD. (B) Wild-type (arrow) and *dhc-1 (RNAi)* (arrowhead) embryos stained with anti–DHC-1 antibodies (top) and counterstained with Hoechst 33258 to reveal DNA (bottom). Anti–DHC-1 staining in this particular *dhc-1 (RNAi)* embryo is 16.3% of that in the neighboring wild-type embryo. Embryos were also stained with antitubulin antibodies to unambiguously identify *dhc-1 (RNAi)* embryos (not shown). (C) Comparison of anti–DHC-1 reactivity in wild-type and *dhc-1 (RNAi)* embryos. On average, 12% of the signal detected in wild-type remains in *dhc-1 (RNAi)* embryos. Bar, 10 μm.

embryos; see Materials and Methods). As shown in Fig. 1, B and C, 88% of the anti–DHC-1 signal was lost on average in *dhc-1 (RNAi)* embryos. Residual staining might be due to incomplete silencing of the *dhc-1* gene by RNAi. Second, we determined that anti–DHC-1 immunostaining was entirely absent from embryos incubated with anti–DHC-1 antibodies in the presence of 0.1 mg/ml DHC-1 peptide (data not shown). Taken together, these results demonstrate that most, if not all, of the signal detected with anti–DHC-1 antibodies in wild-type embryos is specific for the cytoplasmic dynein heavy chain.

Distribution of Cytoplasmic Dynein in Early C. elegans Embryos

We used anti–DHC-1 antibodies to determine the subcellular distribution of cytoplasmic dynein in early wild-type embryos by immunofluorescence microscopy (Fig. 2). We found that cytoplasmic dynein was present in a punctate manner throughout the cytoplasm at all stages of the cell cycle. In addition, a stronger signal was detected at the periphery of pronuclei in one cell stage embryos (Fig. 2 A, arrow and arrowhead) and of nuclei in later stage embryos (Fig. 2 O, black arrowhead). Moreover, cytoplasmic dynein was present at the cell cortex; this was especially apparent at boundaries between cells, for instance, between the AB and P_1 blastomeres of the two cell stage embryo (Fig. 2 O, white arrowheads). The distribution of cytoplasmic dynein changed as cells progressed through mitosis. During prometaphase, cytoplasmic dynein accumulated along both sides of prometaphase chromosomes (Fig. 2, C and D, arrows and arrowhead, respectively). Since chromosomes in *C. elegans* are holocentric (Albertson and Thomson, 1993), this possibly corresponds to kinetochore staining. During metaphase, cytoplasmic dynein became enriched on the spindle (Fig. 2, G–J). During early anaphase (Fig. 2, K–N), strong spindle signal was still detected, both between segregating chromosomes and spindle poles, as well as centrally (Fig. 2 K, arrow), between the two sets of chromosomes (Fig. 2 L, arrowheads). A similar staining pattern persisted throughout anaphase (Fig. 2 O, arrow). At telophase, cytoplasmic dynein was enriched in two areas of the cytoplasm adjacent to the spindle poles (Fig. 2 O, cell to the left). In addition, a strong signal was detected at the periphery of reforming nuclei (Fig. 2 O, black arrowhead).

A subcellular distribution analogous to the one reported here was observed in *C. elegans* embryos using polyclonal antibodies raised against purified dynein heavy chain protein (Lye, J., personal communication). This confirms that the distribution described here truly reflects that of dynein heavy chain and not of an unrelated protein.

Minus End–directed Motility of Yolk Granules Is Abolished in dhc-1 (RNAi) Embryos

We wanted to determine if cytoplasmic dynein function is essential in *C. elegans*. To this end, we specifically silenced the expression of the conventional dynein heavy chain gene *dhc-1* using RNAi. Hermaphrodites were injected with dsRNA corresponding to a segment of the *dhc-1* gene (see Materials and Methods). Such animals gave rise to 100% dead embryos 20 h or more after injection (n = 268 embryos over three experiments). Thus, dynein heavy chain is essential for *C. elegans* embryogenesis. In addition, dynein heavy chain is required for fertility, as mature oocytes ceased being produced 35–40 h after injection.

We addressed whether minus end–directed motor activity was indeed abolished in *dhc-1 (RNAi)* embryos. A manifestation of minus end–directed motility in wild-type one cell stage embryos is the fast movement of yolk granules 0.3–1 μm in diameter towards the center of the asters along linear paths, suggestive of movements along astral microtubules (Fig. 3 A). We determined the average peak velocity of these motility events to be 1.44 μm/s (SD 0.23;

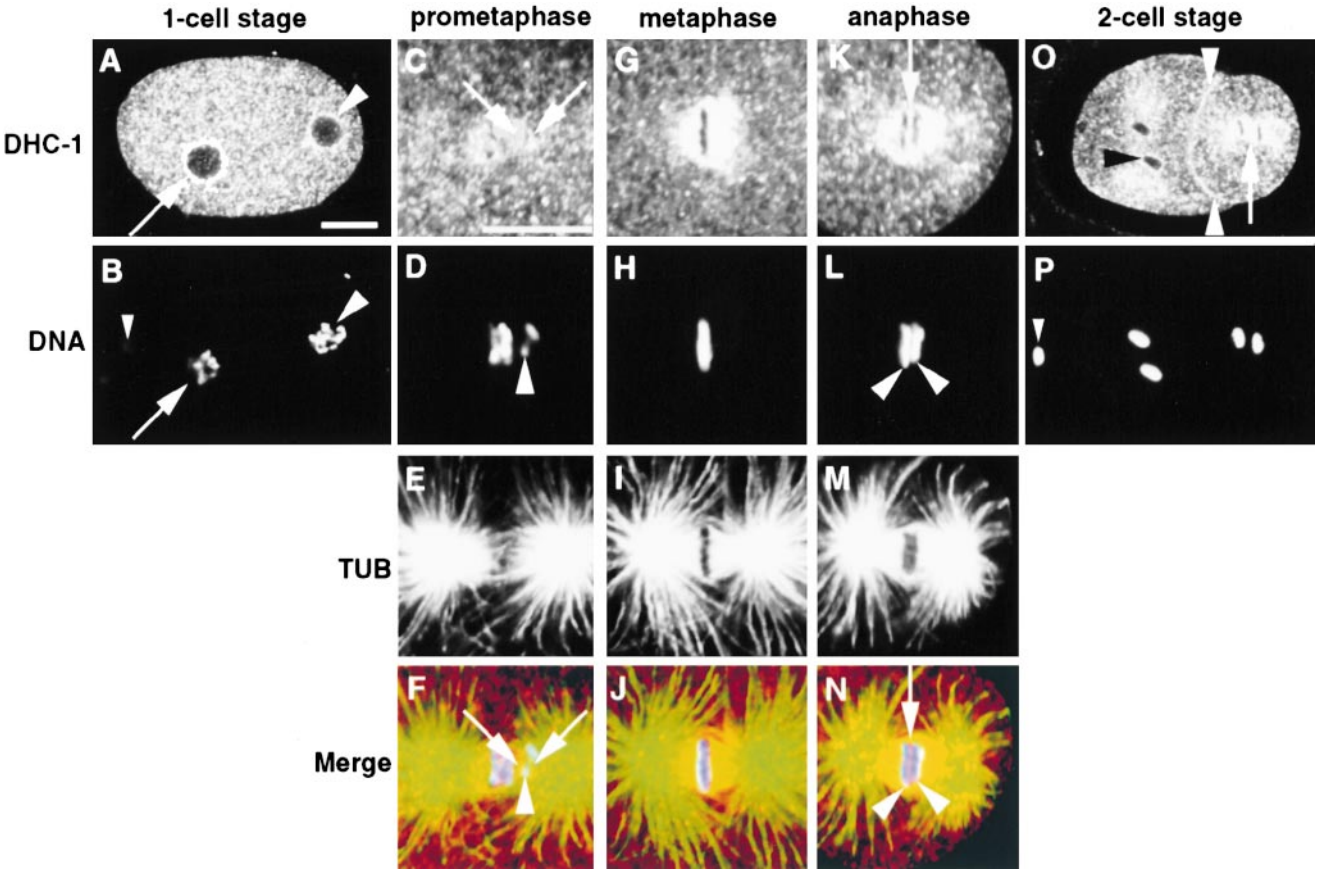

Figure 2. Distribution of cytoplasmic dynein in early wild-type embryos. Embryos stained with anti–DHC-1 and antitubulin (TUB; high magnification images only) antibodies and counterstained with Hoechst 33258 to reveal DNA. A, B, O, and P are at the same magnification, as are C–N. Merged images, DHC-1, red; TUB, green; and DNA, blue. (A and B) One cell stage embryo during pronuclear migration. DHC-1 is distributed throughout the cytoplasm in a punctate manner, and is enriched at the periphery of the male (A and B, arrowhead) and female (A and B, arrow) pronuclei. DHC-1 is also slightly enriched at the cortex of one cell stage embryos, but this is not rendered in this particular focal plane. Small arrowhead in B points to out-of-focus polar body DNA. (C–F) Prometaphase, one cell stage embryo. DHC-1 is enriched on both sides (C and F, arrows) of congressing chromosomes (D and F, arrowhead). (G–J) Metaphase, one cell stage embryo. DHC-1 is enriched on the spindle on both sides of the metaphase plate. (K–N) Early anaphase, P_1 blastomere of two cell stage embryo. DHC-1 is enriched on the spindle between the chromosomes (L and N, arrowheads) and the spindle poles, as well as centrally (K and N, arrow) between the two sets of chromosomes. (O and P) Two cell stage embryo, P_1 blastomere (right) is in late anaphase, AB blastomere (left) in late telophase. In P1, DHC-1 is enriched on the spindle (O, arrow) between the chromosomes and the spindle poles and in the central spindle. In AB, DHC-1 is enriched at the periphery of reforming nuclei (O, black arrowhead) as well as in an area above the spindle poles. In addition, DHC-1 is localized throughout the cortex between the AB and P_1 blastomeres (O, arrowheads). Small arrowhead in P points to polar body DNA. Bars, 10 μm.

Fig. 3 B), which is in the range of velocities that have been reported for dynein-dependent motility events in other systems (e.g., Paschal et al., 1987). During the ~2 min separating the breakdown of the pronuclear envelopes from anaphase, 10 or more such motility events that lasted at least 2 s could be typically observed in a given focal plane in wild-type embryos.

We investigated whether these fast minus end–directed motility events were altered in *dhc-1 (RNAi)* embryos. Of the five *dhc-1 (RNAi)* embryos examined in detail, three displayed no such movement, whereas the remaining two each had a single instance of fast minus end–directed motility event. In contrast to wild-type, however, these two motility events lasted <2 s. The lack of motility events in *dhc-1 (RNAi)* embryos was not merely due to an absence of astral microtubules, as asters in *dhc-1 (RNAi)* embryos were observed both by DIC and immunofluorescence microscopy (see below). Lack of motility events was not due either to a general inability of yolk granule movement because the slower posterior-directed flow of yolk granules that occurs in the cytoplasm of wild-type embryos just before pronuclear migration (Hird and White, 1993) was not affected in *dhc-1 (RNAi)* embryos (Fig. 4 A). Consistent with this observation, segregation of P granules towards the posterior of the embryo, which may be driven by this flow (Strome and Wood, 1983; Hird and White, 1993), was also not affected (32/32 one cell stage *dhc-1 (RNAi)* embryos examined; Fig. 4 B). Taken together, these findings demonstrate that fast minus end–directed motility of yolk granules is specifically abolished in *dhc-1 (RNAi)* embryos and suggest that cytoplasmic dynein drives this form of cellular transport.

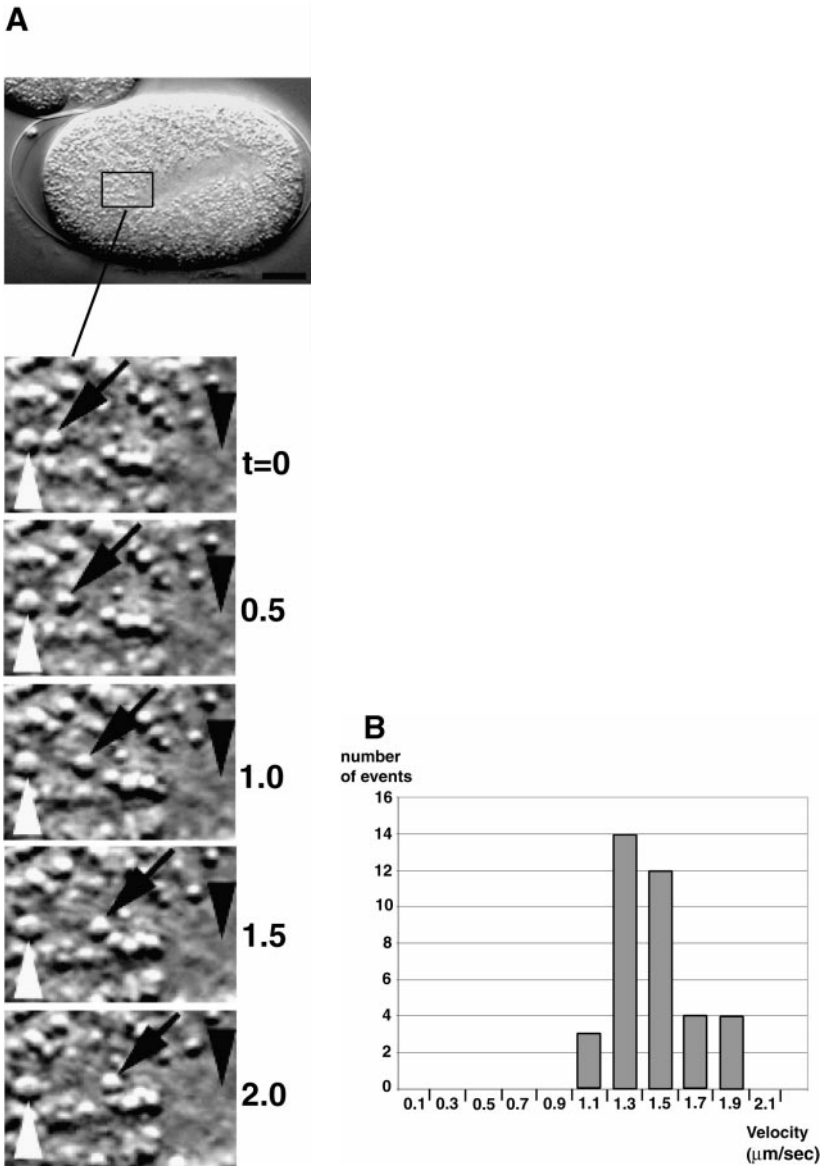

Figure 3. Characterization of rapid minus end–directed movements of yolk granules in wild type. (A) One cell stage embryo in anaphase; high magnification images show an area just anterior of the anterior aster during a 2-s sequence from a time-lapse DIC microscopy recording. Time is indicated in seconds at the right of the frames, which are 10 μm across. One yolk granule (arrows) moves towards the center of the aster (black arrowheads) at an average velocity of 1.40 μm/sec. White arrowheads point to a neighboring yolk granule that remains immobile during the sequence. (B) Histogram of velocities of minus end–directed movement of yolk granules in wild type. Number of motility events per velocity class is shown. Velocity class 1.1 encompasses values from 1.0 to 1.19, velocity class 1.3 values from 1.2 to 1.39 and so forth. On average, motility events (n = 37) lasted 2.7 s (SD 0.85), covered 3.91 μm (SD 1.47), and had a peak velocity of 1.44 μm/s (SD 0.23).

Cytoplasmic Dynein Is Required for Male and Female Pronuclear Migration

To determine the consequences of the loss of cytoplasmic dynein motor activity on MTOC positioning, we examined *dhc-1 (RNAi)* one cell stage embryos by time-lapse DIC microscopy. This approach is well-suited to examine MTOC positioning because yolk granules are excluded from areas of high microtubule density, such as the center of asters and the spindle, as well as from pronuclei and nuclei.

Fig. 5, A–D, shows the relevant sequence of events in wild type. After fertilization, the two meiotic divisions are completed in the one cell stage embryo. The resulting female pronucleus lies slightly off the anterior cortex (Fig. 5 A, left arrow), whereas the male pronucleus is tightly apposed to the posterior cortex (Fig. 5 A, right arrow). The sperm contributes the single centrosome of the one cell stage embryo (Albertson, 1984; Hyman and White, 1987). After duplication, the two daughter centrosomes separate, while remaining closely associated with the male pronucleus. The separated centrosomes migrate slightly anteriorly, along with the male pronucleus, whereas the female pronucleus migrates posteriorly towards the centrosomes. As a result, the male and female pronuclei meet at ~70% egg length (Fig. 5 B; 0% anterior-most, 100% posterior-most).

We found that *dhc-1 (RNAi)* one cell stage embryos displayed several striking phenotypes when examined by time-lapse DIC microscopy (Fig. 5, E–H, and Table I). First, *dhc-1 (RNAi)* embryos often had multiple female pronuclei (Fig. 5 E, three leftmost arrows) and displayed aberrant polar body formation, both indicative of defects during the female meiotic divisions. The role of cytoplasmic dynein during the meiotic divisions is beyond the scope of this work and will not be discussed further here. Second, migration of the male and female pronuclei never took place in *dhc-1 (RNAi)* embryos (Fig. 5 F). The nuclear envelope of the male pronucleus broke down 1–2

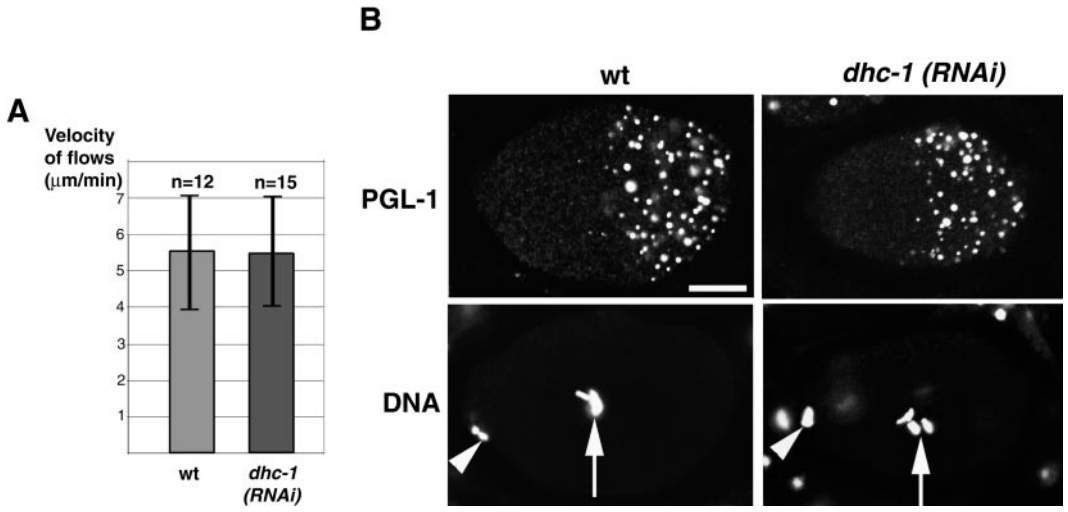

Figure 4. Cytoplasmic flows are not affected in *dhc-1 (RNAi)* embryos. (A) The average peak velocity of posteriorly directed flow of yolk granules during the pseudocleavage stage is indistinguishable in wild type (5.55 μm/min; $n = 12$ granules in 5 embryos; SD 1.63) and *dhc-1 (RNAi)* embryos (5.51 μm/min; $n = 15$ granules in 5 embryos; SD 1.50). These average velocities are slightly higher than those reported previously in wild type (4.4 μm/min; Hird and White, 1993). (B) Wild-type and *dhc-1 (RNAi)* embryos stained with anti–PGL-1 antibodies to visualize P granules and counterstained with Hoechst 33258 to reveal DNA. All images are at the same magnification. In both wild-type and *dhc-1 (RNAi)* one cell stage embryos, PGL-1 is segregated to the posterior. Arrowheads point to anteriorly located polar bodies. The wild-type embryo is in prometaphase (arrow points to chromosomes lining up on the metaphase plate), the *dhc-1 (RNAi)* embryo later in mitosis (arrow points to chromosomes). Embryos were simultaneously stained with antitubulin antibodies (not shown), which revealed the position of centrosomes and unambiguously identified polarity in *dhc-1 (RNAi)* embryos (Fig. 6). Bar, 10 μm.

min before that of the female pronuclei (Fig. 5 G). Such asynchrony is characteristic of mutants defective in pronuclear migration (Gönczy et al., 1999). Third, after breakdown of the pronuclear envelopes, a bipolar spindle was not apparent by DIC microscopy in *dhc-1 (RNAi)* embryos. While an area devoid of yolk granules did extend towards the anterior of the embryo over time (Fig. 5 G, arrow), consistent with an underlying high density of microtubules, no aster was apparent at the anterior end of this area (Fig. 5 G, arrow). Instead, both asters appeared to be located at the very posterior of *dhc-1 (RNAi)* embryos (Fig. 5 G, arrowheads). Fourth, proper cell division did not occur in *dhc-1 (RNAi)* embryos (Fig. 5 H). The absence of cleavage furrow specification was expected given the apparent absence of bipolar spindle. While some furrowing activity did take place towards the anterior of the embryo, this rarely resulted in productive cleavage, like in embryos lacking a spindle after nocodazole treatment (Strome and Wood, 1983). Numerous small nuclei reformed in *dhc-1 (RNAi)* embryos as the cell returned into interphase (Fig. 5 H, arrows), indicative of failure in chromosome segregation. Quicktime movies of a wild-type and a *dhc-1 (RNAi)* embryo can be viewed on the Hyman lab web site (http://www.embl-heidelberg.de/ExternalInfo/hyman/Data.htm) to help compare the sequence of events observed with time-lapse DIC microscopy. In summary, these observations demonstrate that cytoplasmic dynein is essential for pronuclear migration in the one cell stage *C. elegans* embryo. In addition, they suggest a possible role in centrosome separation, since both asters are located together at the very posterior of *dhc-1 (RNAi)* embryos.

Cytoplasmic Dynein Is Required for Centrosome Separation

To test whether centrosome separation was indeed defective in *dhc-1 (RNAi)* embryos, we determined the position of centrosomes by antitubulin staining; in addition, some of the embryos were simultaneously labeled with antibodies against ZYG-9, a centrosomal marker in *C. elegans* (Matthews et al., 1998).

In prophase, daughter centrosomes have separated to opposite sides of the male pronucleus in wild type (Fig. 6 A, arrowheads). In contrast, in *dhc-1 (RNAi)* embryos, daughter centrosomes failed to separate and remained positioned posterior of the male pronucleus (Fig. 6 E, arrowheads). After breakdown of the pronuclear envelopes, the two centrosomes were still in close proximity of one another and located at the very posterior of *dhc-1 (RNAi)* embryos (Fig. 6 M, arrowheads). In contrast to wild type, a bipolar spindle was never observed in *dhc-1 (RNAi)* embryos, and chromosomes were never located in the very small space between centrosomes (46/46 *dhc-1 (RNAi)* embryos examined after breakdown of the male pronucleus). Bundles of microtubules up to 20 μm in length emanated from the posterior where the centrosomes were located and extended anteriorly towards a set of chromosomes (Fig. 6, N and O, arrow). These microtubules most likely correspond to the area devoid of yolk granules that had been observed extending towards the anterior by time-lapse DIC microscopy (Fig. 5 G, arrow). These findings suggest that chromosomes from the male pronucleus are pushed towards the anterior by growing microtubules after breakdown of the pronuclear envelope. Importantly, these results demonstrate that cytoplas-

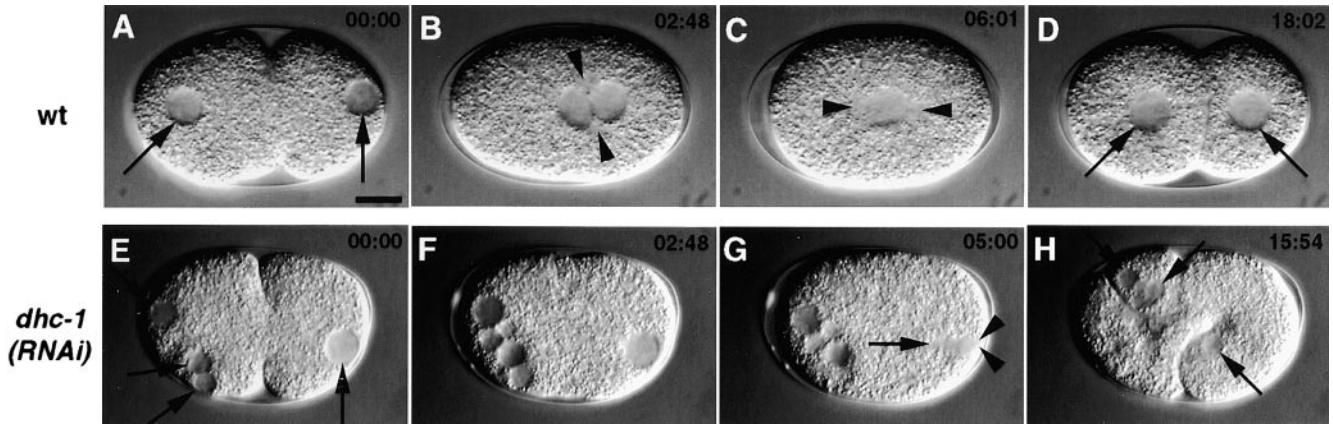

Figure 5. Failure of pronuclear migration in *dhc-1 (RNAi)* embryos. Time-lapse DIC microscopy recordings of wild-type (A–D) and *dhc-1 (RNAi)* embryos (E–H). Time elapsed since the beginning of the sequence is displayed in minutes and seconds in each image. All images are at the same magnification. (A and E) In both wild-type and *dhc-1 (RNAi)* embryo, the male pronucleus is apposed to the posterior cortex (A and E, rightmost arrow). In wild-type, there is a single female pronucleus located slightly off the anterior cortex (A, leftmost arrow). In contrast, there are five female pronuclei in the *dhc-1 (RNAi)* embryo (E, arrows towards the left point at three that are visible in this focal plane). Note the pseudocleavage furrow in the middle of both wild-type and *dhc-1 (RNAi)* embryos. Female pronuclei in some *dhc-1 (RNAi)* embryos were located towards the middle of the embryo (not shown). (B and F) In wild type, after migration of both male and female pronuclei, the pronuclei have met and move along with the centrosome pair (B, arrowheads) towards the center while undergoing a 90° rotation. In contrast, neither male nor female pronuclei migrate in the *dhc-1 (RNAi)* embryo. (C and G) In wild type, the spindle sets up in the cell center and along the longitudinal axis (C, arrowheads point to spindle poles). In the *dhc-1 (RNAi)* embryo, no bipolar structure is visible after nuclear envelope breakdown. However, an area devoid of yolk granules extends towards the anterior of the embryo (arrow in G points to anterior of this area). The asters appear to be at the very posterior of the embryo (G, arrowheads). Note that the membranes of the female pronuclei are still intact after the male pronuclear membrane broke down. (D and H) In wild type, the first cleavage generates two unequally sized daughters, each with a centrally located nucleus (D, arrows). In contrast, no proper cell division occurs in the *dhc-1 (RNAi)* embryo. While some furrowing activity does take place, this is usually restricted to the anterior and does not result in productive cleavage. Numerous small nuclei reform, presumably around nonsegregated chromosomes, as the cell returns into interphase (H, arrows). Bar, 10 μm.

mic dynein is required for centrosome separation in the one cell stage *C. elegans* embryo.

Dynactin Components Are Required for Pronuclear Migration and Centrosome Separation

To confirm that the absence of pronuclear migration and centrosome separation were a result of interfering with cytoplasmic dynein function, we examined the phenotype of embryos depleted of dynactin components by RNAi. Dynactin has been shown to be required for proper cytoplasmic dynein function in several systems (for reviews see Allan, 1994; Schroer et al., 1996). Therefore, silencing of dynactin components by RNAi in *C. elegans* might be expected to result in a similar phenotype to that observed in *dhc-1 (RNAi)* embryos. Contrary to this prediction, however, it has been reported that injection of ssRNA corresponding to the dynactin components p150^{Glued} or p50/dynamitin yield embryos that undergo pronuclear migration and form a bipolar spindle (Skop and White, 1998). However, these embryos may have had residual p150^{Glued} and p50/dynamitin function since ssRNA is much less potent than dsRNA in silencing gene expression (Fire et al., 1998).

Therefore, we tested whether pronuclear migration and centrosome separation were affected after silencing of p150^{Glued} or p50/dynamitin gene expression with dsRNA. As reported in Table I and shown in Fig. 7, A and D, 12/20 *p150^{Glued} (dsRNAi)* and 8/20 *p50/dynamitin (dsRNAi)* embryos had a pronuclear migration phenotype indistinguishable from that of *dhc-1 (RNAi)* embryos by time-lapse DIC microscopy. Like for *dhc-1 (RNAi)* embryos, no bipolar spindle was apparent after breakdown of the pronuclear envelopes in these *p150^{Glued} (dsRNAi)* and *p50/dynamitin (dsRNAi)* embryos, and both asters remained in close proximity to one another at the very posterior of the embryos (Fig. 7, A and D, arrowheads). Staining with antitubulin antibodies confirmed that centrosomes were close to one another at the very posterior of 13/34 *p150^{Glued} (dsRNAi)* and 14/24 *p50/dynamitin (dsRNAi)* embryos examined after breakdown of the male pronucleus (Fig. 7, B and E, arrowheads). The remainder of *p150^{Glued} (dsRNAi)* and *p50/dynamitin (dsRNAi)* embryos had milder phenotypes, resembling in part those obtained after injections of single-stranded material (Skop and White, 1998; Table I). The fact that some *p150^{Glued} (dsRNAi)* and *p50/dynamitin (dsRNAi)* embryos underwent pronuclear migration and centrosome separation may be because of incomplete gene silencing, even by dsRNA. Importantly, these results demonstrate that the dynactin components p150^{Glued} and p50/dynamitin are required, at least in part, for pronuclear migration and centrosome separation in the one cell stage *C. elegans* embryo.

Table I. Summary of Time-lapse DIC Microscopy Analysis

	Number of embryos analyzed	Embryos with single female pronucleus	Embryos with multiple female pronuclei	Average number of multiple female pronuclei*	Defect in pronuclear migration (no bipolar spindle)‡	Defect in pronuclear migration (with bipolar spindle)	Defect in centration/ rotation‖	No apparent defect in one cell stage embryo
N2	20	20	—	NA	—	—	—	20¶
dhc-1 (RNAi)	20	8	12	3 (SD, 0.95)	20**	—	—	—
p150^{Glued} (RNAi)	20	14	6	2 (SD, 0)	12‡‡	2	6§§	—
p50/dynamitin (RNAi)	19	18	2	2 (SD, 0)	8‖‖	2	8¶¶	1

*Average number of multiple female pronuclei among those embryos with multiple female pronuclei. Multiple female pronuclei can be of different sizes; in particular, some are smaller than normal, indicating that they do not contain a full complement of chromosomes.

‡Typical phenotype: both male and female pronuclei fail to migrate. After breakdown of the male pronucleus at the posterior of the embryo, no bipolar spindle is apparent. Consistent with the absence of a functional spindle, there is no cleavage furrow ingression from the posterior of the embryo.

§Typical phenotype: both male and female pronuclei fail to migrate. After breakdown of the male pronucleus at the posterior of the embryo, a bipolar spindle is assembled, although it is typically less apparent than in wild type. Consistent with the presence of a functional spindle, a cleavage furrow ingresses from the posterior of the embryo.

‖Typical phenotype: male and female pronuclei migrate at least to some extent. Subsequent centration of centrosomes and associated pronuclei does not take place; as a consequence, the spindle sets up at ~70% egg length, perpendicular to the longitudinal axis. In most embryos, the spindle remains perpendicular to the longitudinal axis; probably as a consequence, a cleavage furrow ingresses from the posterior of the embryo. In some embryos, spindle orientation is rescued onto the longitudinal axis by the end of anaphase, possibly by the constraints of the eggshell, and the one cell stage embryo divides into two AB-like and P1-like blastomeres.

¶In one embryo, rotation did not take place, while it was incomplete in another one. However, centration was normal in both cases.

**In one embryo, the spindle poles became separated by 2–3 microns by the end of mitosis, although no spindle was apparent between them; probably as a consequence of this separation, a cleavage furrow ingressed from the very posterior of the embryo. In two embryos, the centrosomes were located a few microns away from the male pronucleus; in one of these cases, the two centrosomes were separated to some extent.

‡‡In two embryos, progress through mitosis seemed affected. In one case, the cell spent about 25 min in mitosis (measured from breakdown of the male pronucleus to the reformation of small nuclei), as opposed to approximately 4 min in wild type. In the other case, the cell stayed in mitosis for at least 23 min, after which the recording was interrupted.

§§In one embryo, progress through mitosis seemed affected, as the cell stayed in mitosis for at least 12 min, after which the recording was interrupted.

‖‖In three embryos, the female pronucleus underwent part of its migration, in the absence of male pronuclear migration. In one embryo, the clustered centrosomes were located a few microns away from the male pronucleus. Another embryo spent about 21 min in mitosis.

¶¶In one embryo, rotation took place in the absence of centration.

Cytoplasmic Dynein Is Required, in part, for Maintaining Association between Centrosomes and Pronuclei

Our observations of *dhc-1 (RNAi)* embryos with time-lapse DIC microscopy and indirect immunofluorescence revealed that cytoplasmic dynein is also involved in the mechanisms that maintain centrosome association with nuclei.

In wild-type one cell stage embryos, the separated daughter centrosomes are initially tightly associated with the male pronucleus, and with both pronuclei after pronuclear meeting. This tight association is apparent by DIC microscopy because yolk granules are excluded both from pronuclei and the center of asters (Fig. 8 A, arrows and arrowheads, respectively), as well as by staining with antibodies against tubulin or the centrosomal marker ZYG-9 (Fig. 8 B, arrowheads) and counterstaining with Hoechst 33258 to visualize DNA (Fig. 8 B, arrow).

While the majority of *dhc-1 (RNAi)* embryos maintained association between the unseparated centrosomes (Fig. 8, C and D, arrowheads) and the male pronucleus (Fig. 8, C and D, arrow), this was not always the case. In ~15% of *dhc-1 (RNAi)* embryos (7/45 embryos in prophase analyzed by antitubulin antibodies and Hoechst 33258), the centrosomes were not in the immediate vicinity of the male pronucleus (Fig. 8, E and F, arrow), but instead located 3–11 μm away (average 6.1 μm, SD 2.63; Fig. 8, E and F, arrowheads). In addition, we noted that centrosomes remained at the posterior cortex in these embryos (Fig. 8, E and F, arrowheads), even though the male pronucleus was not present anterior to them. This suggests that cytoplasmic dynein is required for movement of centrosomes away from the posterior cortex.

These results indicate that cytoplasmic dynein is required, at least in part, for proper association between centrosomes and the male pronucleus in the one cell stage *C. elegans* embryo. Cytoplasmic dynein appears to play a role in maintaining this association, rather than in establishing it, because asters initially in close proximity to the male pronucleus can be observed drifting away in time-lapse DIC recordings of *dhc-1 (RNAi)* embryos (data not shown).

Cytoplasmic Dynein Is Required for Proper Spindle Orientation in the One Cell Stage Embryo

We wanted to test whether cytoplasmic dynein is required for the positioning of centrosomes onto the longitudinal axis that leads to proper spindle orientation in the one cell stage *C. elegans* embryo. However, the lack of centrosome separation in *dhc-1 (RNAi)* embryos precludes addressing this question because of the resulting absence of spindle assembly. Therefore, we sought to generate weaker phenotypes with RNAi to bypass the early requirement for centrosome separation.

Weaker phenotypes were produced by injecting undiluted ssRNA and examining embryos 12–16 h after injection or by injecting 16-fold diluted ssRNA and examining embryos 24–30 h after injection. The resulting *dhc-1 (ssRNAi)* embryos reproducibly fell into one of three broad phenotypic classes, corresponding to the equivalent of an allelic series. First, embryos that were wild type. In these cases, the RNAi effect was probably too weak to significantly deplete dynein heavy chain. Second, embryos that had phenotypes akin to those obtained after injection of double-stranded material. In these cases, the RNAi effect was probably strong enough to deplete a substantial fraction of dynein heavy chain. Third, embryos that exhibited milder phenotypes that probably resulted from intermediate dim-

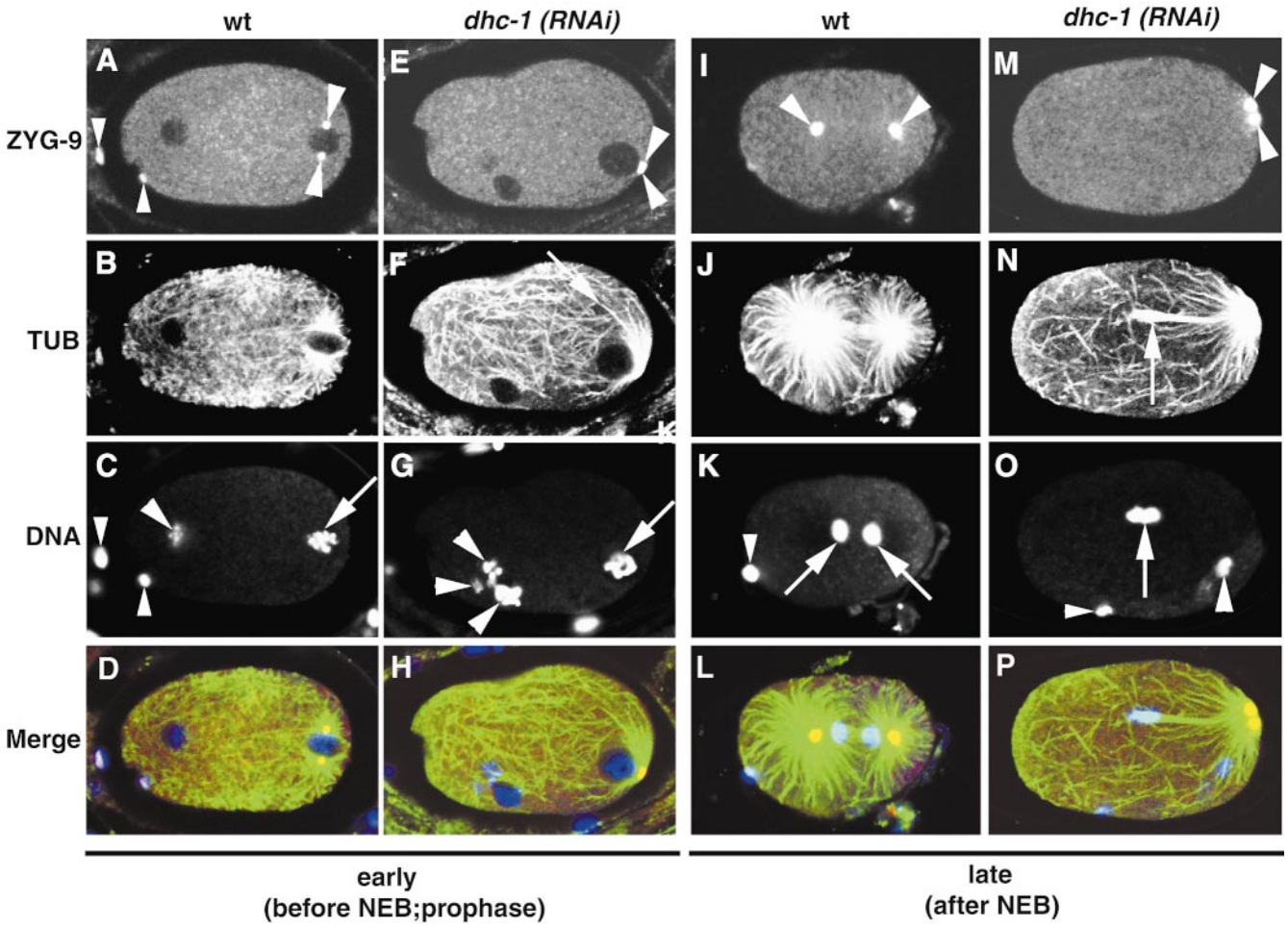

Figure 6. Failure of centrosome separation in *dhc-1 (RNAi)* embryos. Embryos stained with anti–ZYG-9 and antitubulin (TUB) antibodies and counterstained with Hoechst 33258 to reveal DNA. Images in first two columns: early, before nuclear envelope breakdown (NEB); and prophase. Images in last two columns: late, after NEB. Merged images: ZYG-9, red; TUB, green; and DNA, blue. All images are at the same magnification. (A–D) Wild type, prophase. (A) ZYG-9 labels the two centrosomes (arrowheads), which have separated from one another while remaining associated with the male pronucleus; ZYG-9 is also present in the cytoplasm and polar bodies (small arrowheads). (B) Astral microtubules emanate from the centrosomes; the mesh of cortical microtubules is also visible. (C) DNA of both male (arrow) and female (out of focus, arrowhead) pronuclei is condensing; small arrowheads point to polar body material. (E–F) *dhc-1 (RNAi)*, prophase. (E) Daughter centrosomes (arrowheads) fail to separate from one another and are posterior of the male pronucleus. (F) Some astral microtubules are fairly long (arrow). (G) DNA of both the male (arrow) and the three female (arrowheads) pronuclei is condensing. (I–L) Wild type, anaphase. (I) The two spindle poles (arrowheads) have moved away from each other during anaphase B. (J) Numerous and long astral microtubules extend from the spindle poles towards the anterior and posterior cortices; spindle microtubules extend centrally. (K) The two sets of chromosomes segregate towards the spindle poles; small arrowhead points to polar body material. (M–P) *dhc-1 (RNAi)*; after NEB. (M) Centrosomes (arrowheads) are still in close proximity of one another. (N) No bipolar spindle is assembled; astral microtubules seem to grow preferentially towards chromosomes or be stabilized in their vicinity (arrow); such microtubules are directed towards chromosomes coming presumably from the male pronucleus in most *dhc-1 (RNAi)* embryos. (O) Condensed chromosomes coming most likely from the male pronucleus (arrow) and the female pronucleus (arrowhead) are visible. Small arrowhead points to laterally positioned polar body material. In 1/46 *dhc-1 (RNAi)* embryo after NEB, the two centrosomes were separated from one another; a bipolar spindle was not apparent in this case either. Bar, 10 μm.

inution of cytoplasmic dynein function; MTOC positioning in embryos of the third class is described below.

In wild type, the centrosome pair is positioned at 70% egg length and transverse to the longitudinal axis after pronuclear meeting (Fig. 9 A, arrowheads). The centrosome pair and associated pronuclei subsequently move to the embryo center while undergoing a 90° rotation (Fig. 9 B, arrowheads). As a result, after breakdown of the pronuclear envelopes, the spindle is positioned in the cell center and oriented along the longitudinal axis (Fig. 9 C, arrowheads).

We found that the third class of *dhc-1* (ssRNAi) embryos underwent pronuclear migration as in wild type (compare Fig. 9, A and D), but failed to undergo subsequent centration and rotation of centrosomes (compare Fig. 9, B and E). As a result, the spindle was set up at ~70% egg length, perpendicular to the longitudinal axis (Fig. 9 E). However, the spindle was typically rescued onto

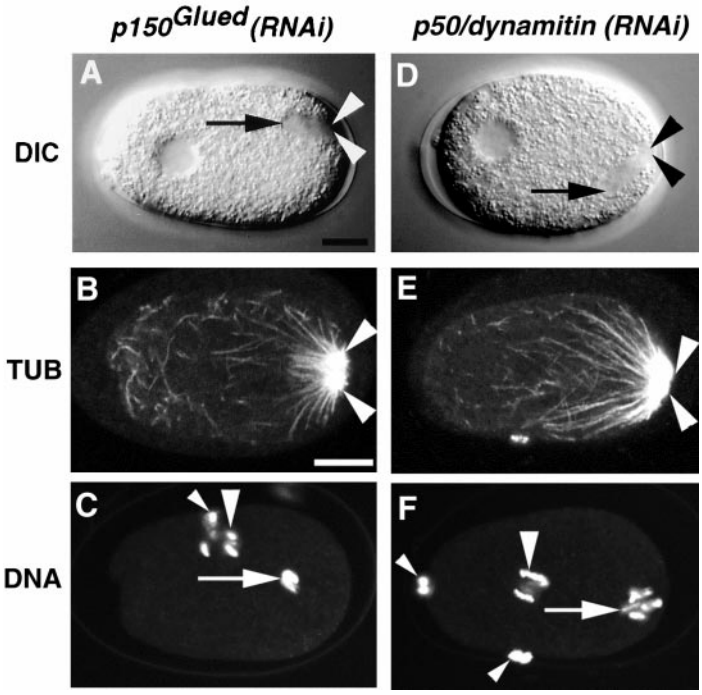

Figure 7. Failure of pronuclear migration and MTOC separation in *p150^{Glued} (RNAi)* and *p50/dynamitin (RNAi)* embryos. (A and D) Single images from time-lapse DIC microscopy recordings of *p150^{Glued} (RNAi)* (A) and *p50/dynamitin (RNAi)* (D) embryos. (B, C, E, and F) *p150^{Glued} (RNAi)* (B and C) and *p50/dynamitin (RNAi)* embryos (E and F) stained with antitubulin antibodies and counterstained with Hoechst 33258 to reveal DNA. A and D are at the same magnification, as are B, C, E, and F. (A and D) In both *p150^{Glued} (RNAi)* and *p50/dynamitin (RNAi)* embryos, no bipolar spindle is visible after NEB. However, an area devoid of yolk granules extends towards the anterior of the embryo (arrows point to anterior of this area). The asters appear to be at the very posterior of the embryos (arrowheads). Note that the membranes of the female pronuclei are still intact after that of the male pronuclei broke down. (B, C, E, and F) In both *p150^{Glued} (RNAi)* and *p50/dynamitin (RNAi)* embryos, the two MTOCs are in close proximity at the very posterior of the embryo (B and E, arrowheads). *p150^{Glued} (RNAi)* embryo is just after breakdown of the male pronucleus (C, arrow); arrowhead in C points to condensed chromosomes from the female pronucleus. *p50/dynamitin (RNAi)* embryo is towards the end of prophase, before breakdown of the male pronucleus. At these stages in wild type, centrosomes are well separated (Fig. 6). Small arrowheads in C and F point to polar body material. Bars, 10 μm.

the longitudinal axis by the end of anaphase, presumably because of the physical constraints of the eggshell (Fig. 9 F). An identical phenotype has been reported previously for *p150^{Glued} (ssRNAi)* and *p50/dynamitin (ssRNAi)* embryos (Skop and White, 1998), and was observed in this study for some *p150^{Glued} (dsRNAi)* and *p50/dynamitin (dsRNAi)* embryos (Table I). These results demonstrate that cytoplasmic dynein, like dynactin components, is required for centration/rotation of centrosomes and, thus, proper spindle orientation, in the one cell stage *C. elegans* embryo.

Discussion

By using RNAi, we have demonstrated that cytoplasmic dynein is required for all three major aspects of centrosome positioning that occur in the one cell stage *C. elegans* embryo: centrosome separation, movement of centrosomes away from the posterior cortex accompanying male pronuclear migration, and subsequent positioning of centrosomes onto the longitudinal axis. In addition, we found that cytoplasmic dynein is required for female pronuclear migration and plays a role in maintaining association between centrosomes and male pronucleus.

Using RNAi to Analyze the Function of Cytoplasmic Dynein

The function of cytoplasmic dynein in MTOC positioning in complex eukaryotes has not been unambiguously determined in the past, owing largely to experimental difficulties associated with loss-of-function studies. Both in *Drosophila* and mice, cells bearing strong mutations in the heavy chain gene fail to proliferate or survive (Gepner et al., 1996; Harada et al., 1998), severely hampering investigation of cytoplasmic dynein function.

Such difficulties can be circumvented by using RNAi in *C. elegans*. Germ cells targeted by RNAi undergo no divisions between the time of injection and fertilization. Therefore, even if cytoplasmic dynein is essential for an aspect of cell division, this alone cannot interfere with analyzing its function in the one cell stage embryo. Cytoplasmic dynein does play a role during the meiotic divisions that take place shortly after fertilization, since *dhc-1 (RNAi)* one cell stage embryos often possess multiple female pronuclei. However, this does not prevent scoring cell division processes in the remainder of the first cell cycle, and cannot explain the subsequent defects of centrosome positioning. Indeed, the same defects are observed in those *dhc-1 (RNAi)* embryos that have a single female pronucleus. Conversely, centrosome positioning defects are not apparent in a number of mutant strains with multiple female pronuclei (Gönczy et al., 1999).

One potential limitation of using RNAi resides in the possibility that the component under study is also required to generate mature oocytes, in which case function in the one cell stage embryo may not be assessed. In fact, cytoplasmic dynein does play some role in gametogenesis, since oocyte production ceases 35–40 h after injection of *dhc-1* dsRNA. Nonetheless, this has not hampered our analysis, because reproducible phenotypes were observed in one cell stage embryos 24–32 h after injection. Therefore, RNAi in *C. elegans* offers an excellent opportunity to analyze the in vivo requirements of cytoplasmic dynein in MTOC positioning in a complex eukaryote.

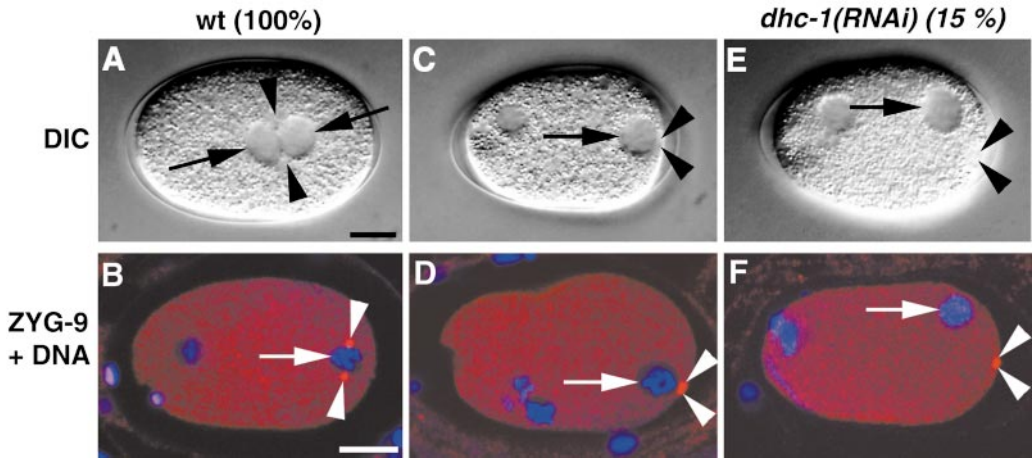

Figure 8. Centrosomes and male pronucleus are not tightly associated in some *dhc-1 (RNAi)* embryos. (A, C, and E) Time-lapse DIC microscopy of wild-type (A) and *dhc-1 (RNAi)* embryos (C and E). A is from the wild-type embryo shown in Fig. 5. (B, D, and F) Wild-type (B) and *dhc-1 (RNAi)* embryos (D and F) stained with anti–ZYG-9 antibodies and counterstained with Hoechst 33258 to reveal DNA. B and D are from embryos shown in Fig. 6. Merged images, ZYG-9, red; DNA, blue. A, C, and E are at the same magnification, as are B, D, and F. (A and B) In wild type, centrosomes are initially associated with the male pronucleus, and with both male and female pronuclei after pronuclear meeting. (A) The center of the asters is visible by DIC microscopy as areas excluding yolk granules (arrowheads); arrows point to associated pronuclei. (B) Anti–ZYG-9 labeling demonstrates that the two centrosomes (arrowheads) are associated with the male pronucleus (arrow). (C and D) In 85% of *dhc-1 (RNAi)* embryos, unseparated centrosomes are in the immediate vicinity of the male pronucleus. (C) An area lacking yolk granules and corresponding to the center of the asters (arrowheads) is visible just posterior of the male pronucleus (arrow). (D) Anti–ZYG-9 labeling demonstrates that unseparated centrosomes (arrowheads) are located in the immediate vicinity and posterior of the male pronucleus (arrow). (E and F) In 15% of *dhc-1 (RNAi)* embryos, unseparated centrosomes are located 3–11-μm away from the male pronucleus. (E) The area lacking yolk granules and corresponding to the center of the asters (arrowheads) is located 6.5 μm away from the male pronucleus (arrow) in this particular embryo. (F) Anti–ZYG-9 labeling reveals that unseparated centrosomes (arrowheads) are located 7.94-μm away from the male pronucleus (arrow) in this particular embryo. In 1 of 7 embryos where association was compromised, the two centrosomes were separated from one another, and only one of them was not associated with the male pronucleus. Although the embryo shown in F is too early in the cell cycle to be unambiguously scoreable for the occurrence of centrosome duplication, there were two centrosomes in 91/91 one cell stage *dhc-1 (RNAi)* embryos examined during prophase or after NEB. Bars, 10 μm.

Cytoplasmic Dynein May Be Generally Required for Centrosome Separation in Metazoans

Our results unequivocally establish that cytoplasmic dynein and dynactin are required for centrosome separation in the one cell stage *C. elegans* embryo. A similar conclusion had been reached for cytoplasmic dynein from experiments in vertebrate cells that made use of function-blocking antibodies (Vaisberg et al., 1993). However, subsequent studies suggested that dynein and dynactin are not needed for centrosome separation (Echeverri et al., 1996; Gaglio et al., 1997). These apparently conflicting data may be reconciled if the majority of cells in the later studies retained sufficient motor activity to permit centrosome separation and proceed through to subsequent stages of mitosis, where there may be a higher requirement for dynein and dynactin function. Interestingly, cytoplasmic dynein is not required for MTOC separation in *S. cerevisiae* (Eshel et al., 1993; Li et al., 1993). Therefore, whereas many cell division processes have been conserved throughout evolution of eukaryotic cells, the use of cytoplasmic dynein to separate MTOCs may be specific to metazoans. Perhaps different mechanisms of MTOC separation have been imparted by the fact that spindle pole bodies are embedded in the nuclear envelope, in contrast to centrosomes that are simply associated with nuclei.

Mechanisms of Dynein-dependent Separation of Centrosome

Two conditions must be met for proper centrosome separation to take place in complex eukaryotes. First, centrosomes must move until they are diametrically opposed on the nucleus. Second, separating centrosomes must remain tightly associated with the nucleus. Two types of mechanisms have been invoked to explain centrosome separation. In one, separation results from pushing forces acting on overlapping antiparallel microtubules emanating from the two centrosomes. Plus end–directed motors are expected to generate the force driving separation in this case. The requirement for plus end–directed kinesins like Xklp2 in centrosome separation lends support to this view (Boleti et al., 1996). A minus end–directed motor such as cytoplasmic dynein may still be essential in this scenario by transporting effector molecules like Xklp2 (Wittman et al., 1998). However, this type of mechanism requires the existence of an extranuclear spindle during centrosome separation, which has not been observed in several vertebrate cells or in the *C. elegans* embryo (Roos, 1973; Rattner and Berns, 1976; Bajer and Mole-Bajer, 1982; Albertson, 1984; Hyman and White, 1987). Moreover, this type of mechanism predicts that centrosomes move apart in a coordinated fashion, whereas there is evidence to the con-

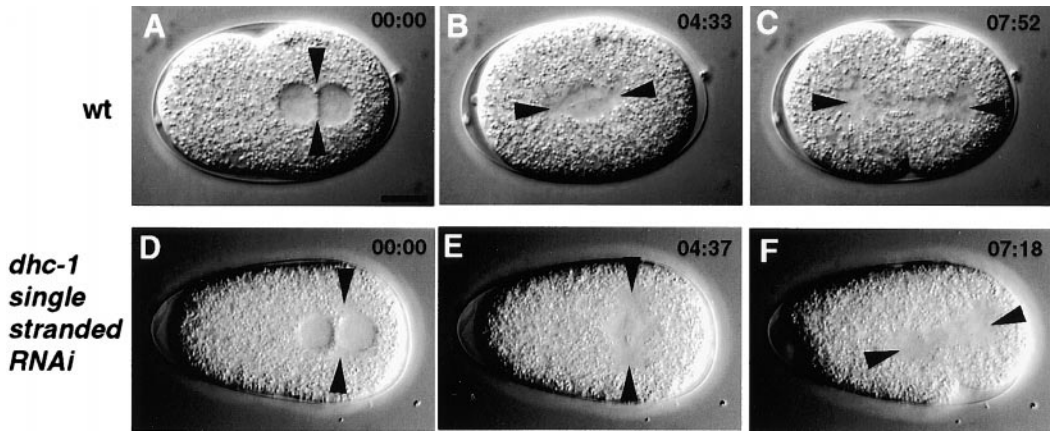

Figure 9. Spindle orientation defect in *dhc-1 (ssRNAi)* embryos. Time-lapse DIC microscopy recordings of wild-type (A–C) and *dhc-1 (ssRNAi)* (D–F) embryos. In each image, time elapsed since the beginning of the sequence is displayed in minutes and seconds and arrowheads point to center of asters and spindle poles. All images are at the same magnification. (A and D) In both wild-type and *dhc-1 (ssRNAi)* embryos, pronuclei meet at ~70% egg length. (B and E) In wild type, the centrosome pair and associated pronuclei move towards the center while undergoing a 90° rotation. This does not happen in the *dhc-1 (ssRNAi)* embryo. As a result, while the spindle sets up in the cell center and along the longitudinal axis in wild-type, it does so in the posterior half and perpendicular to the longitudinal axis in the *dhc-1 (ssRNAi)* embryo. (C and F) Both wild-type and *dhc-1 (ssRNAi)* embryos divide asymmetrically into a larger anterior blastomere and a smaller posterior one. In the *dhc-1 (ssRNAi)* embryo, this occurs after rescue of the spindle orientation onto the longitudinal axis during anaphase, possibly because of the physical constraints of the eggshell. Note that the cleavage furrow ingresses sooner on one side of the *dhc-1 (ssRNAi)* embryo (bottom side), because the spindle was closer to that side during rescue of spindle orientation. In some *dhc-1 (ssRNAi)* embryos, >1 nucleus reformed in each daughter blastomere, indicative of defects in chromosome segregation. Bar, 10 μm.

trary in newt cells (Waters et al., 1993). Finally, such a mechanism alone does not explain how separating centrosomes remain tightly associated with the nucleus.

In the second type of mechanism, separation results from pulling forces acting on astral microtubules in front of the moving centrosomes. Minus end–directed motors are expected to generate the force driving separation in this case. The requirement for cytoplasmic dynein uncovered in this study is fully compatible with this view. Dynein could generate such pulling forces by being anchored throughout the cytoplasm or at the cell cortex, as has been discussed previously (Vaisberg et al., 1993). Here, we propose an alternative model in which pulling forces result from interactions between cytoplasmic dynein anchored on the nucleus and astral microtubules (Fig. 10). Supporting evidence for such a model comes from the presence of cytoplasmic dynein at the periphery of nuclei, both in MDCK cells and in *C. elegans* (Busson et al., 1998; this work). This model is attractive because it provides a single mechanism to explain both how centrosome separate and how they remain tightly associated with the nucleus.

While we have no direct data to support this model at present, evidence that interactions between cytoplasmic dynein anchored on nuclei and astral microtubules can generate force comes from our discovery that female pronuclei fail to migrate in *dhc-1 (RNAi)* embryos. In wild type, cytoplasmic dynein is enriched at the periphery of the female pronucleus, and may, thus, drive migration of this organelle toward centrosomes by minus end–directed motility. Additional evidence compatible with this mechanism comes from *Xenopus* in which a reconstituted system that mimics female pronuclear migration has been shown to require cytoplasmic dynein function (Reinsch and Karsenti, 1997).

Why would centrosomes in the model presented in Fig. 10 move apart until they are diametrically opposed to one another? The role of cytoplasmic dynein suggests a possible mechanism involving length-dependent forces. In this scenario, the minus ends of astral microtubules, along with the centrosome, are pulled when they encounter anchored cytoplasmic dynein on the nucleus. Longer astral microtubules encounter more anchored motors and, thus, experience a stronger pulling force than shorter ones. After centrosome duplication, microtubules extending away from the centrosomes along the nucleus are long, whereas those projecting towards the other centrosome are short. Thus, length-dependent forces could ensure that centrosomes move away from each other until such pulling forces are balanced, which occurs when they are diametrically opposed. In this model, the initial position of daughter centrosomes after duplication determines the final position of separated centrosomes.

Such a mechanism for centrosome separation would simultaneously ensure association between separating centrosomes and the nucleus. The nature of the association between centrosomes and nuclei is poorly understood. It has been postulated that organelle-like motility of nuclei along microtubules may serve to maintain this association (Reinsch and Gönczy, 1998). The presence of cytoplasmic dynein on nuclei in MDCK cells and in *C. elegans* is compatible with this postulate (Busson et al., 1998; this work). Importantly, our finding that the association between centrosomes and male pronucleus is lost in some *dhc-1 (RNAi)* embryos provides the first evidence that cytoplas-

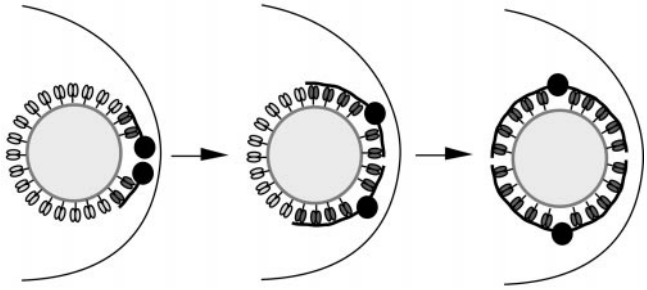

Figure 10. Possible model of dynein-dependent separation of centrosomes. View is on posterior of one cell stage embryo. Male pronucleus: large light disk. Centrosomes: small black disks. Shown also are astral microtubules (black lines) and two-headed cytoplasmic dynein; cytoplasmic dynein molecules that interact with astral microtubules are shown in dark shading, others in light shading. Cytoplasmic dynein is evenly distributed on the male pronucleus. When astral microtubules encounter such anchored motors, their minus end is pulled towards cytoplasmic dynein, along with the centrosome. Longer astral microtubules encounter more motors and, thus, experience a stronger pulling force than shorter ones. Because astral microtubules growing towards the anterior are longer to start with, dynein-dependent forces displace centrosomes towards the anterior initially. When astral microtubules growing in all directions along the nuclear envelope are of equal size, centrosome movement stops. In this model, cytoplasmic dynein also serves to couple male pronucleus and centrosomes. See text for additional information.

mic dynein may indeed play a role in maintaining the nucleus tightly associated with centrosomes by minus end–directed motility.

Cytoplasmic Dynein Function in Centrosome Movement Away from the Cortex

We have shown that cytoplasmic dynein and dynactin are required for the movement of centrosomes away from the posterior cortex that accompanies male pronuclear migration. Perhaps centrosomes remain at the posterior cortex in the absence of cytoplasmic dynein function as a secondary consequence of defective separation. In wild type, microtubule polymerization forces that act against the posterior cortex are thought to push away centrosomes and associated male pronucleus (Albertson, 1984). In the absence of centrosome separation, perhaps the close proximity of two MTOCs somehow prevents microtubule polymerization forces from efficiently acting against the posterior cortex. Another possibility is that movement of centrosomes away from the posterior cortex occurs via pulling forces exerted by dynein anchored throughout the cytoplasm.

Cytoplasmic Dynein Is Required for Spindle Orientation in the One Cell Stage C. elegans Embryo

Separated centrosomes alter their position before spindle assembly in many cells, thus ensuring proper spindle orientation during mitosis (for reviews see Gönczy and Hyman, 1996; Strome and White, 1996; Jan and Jan, 1998). In the wild-type one cell stage *C. elegans* embryo, centration/rotation of centrosomes ensures that the spindle sets up along the longitudinal axis. By using ssRNA to bypass the requirement for centrosome separation, we found that centration/rotation and spindle orientation in the one cell stage embryo require cytoplasmic dynein function. A similar result is obtained when $p150^{Glued}$ or p50/dynamitin are subjected to weak RNAi effects (Skop and White, 1998; this work).

Cytoplasmic dynein and dynactin are also required for proper orientation of the spindle at the bud neck in *S. cerevisiae* (Eshel et al., 1993; Li et al., 1993; Clark and Meyer, 1994; Muhua et al., 1994). It has been proposed that dynactin at the bud cortex tethers cytoplasmic dynein, which captures astral microtubules and translocates the associated spindle pole body by minus end–directed motility towards the bud neck (for review see Gönczy and Hyman, 1996). An analogous cortical capture mechanism could account for centration/rotation in the one cell stage *C. elegans* embryo, if cytoplasmic dynein were tethered somewhere in the anterior of the embryo. We have shown that cytoplasmic dynein is present at the cortex of one cell stage embryos, albeit at low levels. Since $p150^{Glued}$ is enriched at the site of polar body extrusion, at the very anterior cortex (Skop and White, 1998), it is formally possible that cytoplasmic dynein at this site mediates centration/rotation. However, we think this is unlikely because this process still occurs in rare embryos in which polar bodies are positioned away from the anterior cortex (Gönczy, P., unpublished observations). Evidence from *S. cerevisiae* suggests an alternative to the cortical capture model. In this organism, microtubule dynamics are affected in dynein heavy chain mutants, and the average length of microtubules is altered in mutants of other motor proteins that play a role in spindle orientation (Cottingham and Hoyt, 1997; DeZwaan et al., 1997; Shaw et al., 1997). While the exact role of microtubule dynamics in *S. cerevisiae* spindle orientation remains to be determined, these observations raise the possibility that cytoplasmic dynein could similarly influence microtubule dynamics in *C. elegans*. This, in turn, may be responsible for some of the phenotypic manifestations reported in this work, including improper spindle orientation in the one cell stage embryo.

Spindle Orientation in P_1 with Reduced Cytoplasmic Dynein or Dynactin Function

Separated centrosomes in the P_1 blastomere of the two cell stage *C. elegans* embryo also undergo a 90° rotation that aligns them along the longitudinal axis. It has been suggested that P_1 rotation also results from a cortical capture mechanism (Hyman and White, 1987). In this case, laser microsurgery experiments identified the requirement for a discrete cortical site, which overlaps with the cell division remnant generated after cleavage of the one cell stage embryo (Hyman, 1989). The dynactin components actin capping protein and $p150^{Glued}$ are enriched at this site, lending support to the hypothesis that cytoplasmic dynein anchored at this site drives P_1 rotation (Waddle et al., 1994; Skop and White, 1998). Compatible with this view, we found that cytoplasmic dynein is present all along the cortex in the P_1 blastomere, including the cortical site.

However, despite this correlative finding, we could

not assess the role of cytoplasmic dynein in P_1 rotation with certainty. While P_1 rotation was defective in some *dhc-1 (ssRNAi)* embryos (Gönczy, P., S. Pichler, and M. Kirkham, unpublished observations), this may not reflect a direct requirement for cytoplasmic dynein function. Indeed, the first cleavage furrow typically ingressed sooner on one side of *dhc-1 (ssRNAi)* embryos after rescue of spindle orientation onto the longitudinal axis (Fig. 9 F). As a result, the cortical site is predicted to be eccentrically located. A similar asynchronous ingression of the first cleavage furrow has been observed in weak *p150^{Glued} (RNAi)* and *p50/dynamitin (RNAi)* embryos (Skop and White, 1998). In this case, eccentric location of the cortical site has been directly demonstrated by anti-p150^{Glued} staining in *p50/dynamitin (ssRNAi)* embryos (Skop and White, 1998). Therefore, we suggest that the failure of P_1 rotation with diminished cytoplasmic dynein or dynactin function may result from the eccentric location of the cortical site caused by asynchronous ingression of the first cleavage furrow. We believe that demonstration of a direct requirement of cytoplasmic dynein and dynactin function in P_1 rotation awaits further experiments, including the use of temperature-sensitive alleles or local inactivation of protein function. The development of such experimental approaches will be important to further dissect the requirement of cytoplasmic dynein in *C. elegans* and other metazoans where RNAi is not available.

Special thanks to John Lye (University of Virginia, Charlottesville, VA) for having shared with us his results about the distribution of dynein heavy chain in *C. elegans* embryos. We thank Yuji Kohara for providing cDNAs, Fabio Piano (Cornell University, Ithaca, NY) for advice on phage PCR and Alan Coulson for generating dsRNAs. We are grateful to Lisa Matthews (Cornell University, Ithaca, NY) for anti–ZYG-9 antibodies, Susan Strome (Indiana University, Bloomington, IN) for anti–PGL-1 antibodies and Sigrid Reinsch for anti-*Xenopus* dynein heavy chain antibodies. For help in improving the manuscript, we thank Arshad Desai, Chris Echeverri, Michael Glotzer (IMP, Vienna, Austria), Karen Oegema, and Eric Karsenti (all from EMBL, Heidelberg, Germany).

Work in the Hyman laboratory is supported by the European Molecular Biology Laboratory and the Max-Planck Institute. Pierre Gönczy was a fellow from the European Molecular Biology Organization (ATLF 787-1995), the Human Frontier Science Program (LT-202/96), and the Swiss National Science Foundation (TMR 83EU-045376) during parts of this project.

Submitted: 15 April 1999
Revised: 18 August 1999
Accepted: 23 August 1999

Note Added in Proof. Defects in centrosome separation and in the association between centrosomes and nuclei also have been recently described in *Drosophila* embryos with reduced cytoplasmic dynein function (Robinson, J.T., E.J. Wojcik, M.A. Sanders, M. McGrail, and T.S. Hays. *J. Cell Biol.* 146:597–608).

References

Albertson, D. 1984. Formation of the first cleavage spindle in nematode embryos. *Dev. Biol.* 101:61–72.

Albertson, D.G., and J.N. Thomson. 1993. Segregation of holocentric chromosomes at meiosis in the nematode, *Caenorhabditis elegans*. *Chromosome Res.* 1:15–26.

Allan, V. 1994. Organelle movement. Dynactin: portrait of a dynein regulator. *Curr. Biol.* 4:1000–1002.

Bajer, A.S., and J. Mole-Bajer. 1982. Asters, poles, and transport properties within spindlelike microtubule arrays. *Cold Spring Harb. Symp. Quant. Biol.* 1:263–283.

Boleti, H., E. Karsenti, and I. Vernos. 1996. XKLP2, a novel *Xenopus* centrosomal kinesin-like protein required for centrosome separation during mitosis. *Cell.* 84:49–59.

Burkhardt, J.K., C.J. Echeverri, T. Nilsson, and R.B. Vallee. 1997. Overexpression of the dynamitin (p50) subunit of the dynactin complex disrupts dynein-dependent maintenance of membrane organelle distribution. *J. Cell Biol.* 139:469–484.

Busson, S., D. Dujardin, A. Moreau, J. Dompierre, and J.R. De Mey. 1998. Dynein and dynactin are localized to astral microtubules and at cortical sites in mitotic epithelial cells. *Curr. Biol.* 8:541–544.

Clark, S.W., and D.I. Meyer. 1994. ACT3: a putative centractin homologue in *S. cerevisiae* is required for proper orientation of the mitotic spindle. *J. Cell Biol.* 127:129–138.

Corthesy-Theulaz, I., A. Pauloin, and S.R. Rfeffer. 1992. Cytoplasmic dynein participates in the centrosomal localization of the Golgi complex. *J. Cell Biol.* 118:1333–1345.

Cottingham, F.R., and M.A. Hoyt. 1997. Mitotic spindle positioning in *Saccharomyces cerevisiae* is accomplished by antagonistically acting microtubule motor proteins. *J. Cell Biol.* 138:1041–1053.

DeZwaan, T.M., E. Ellingson, D. Pellman, and D.M. Roof. 1997. Kinesin-related KIP3 of *Saccharomyces cerevisiae* is required for a distinct step in nuclear migration. *J. Cell Biol.* 138:1023–1040.

Echeverri, C.J., B.M. Paschal, K.T. Vaughan, and R.B. Vallee. 1996. Molecular characterization of the 50-kD subunit of dynactin reveals function for the complex in chromosome alignment and spindle organization during mitosis. *J. Cell Biol.* 132:617–634.

Eshel, D., L.A. Urrestarazu, S. Vissers, J.C. Jauniaux, J.C. van Vliet-Reedijk, R.J. Planta, and I.R. Gibbons. 1993. Cytoplasmic dynein is required for normal nuclear segregation in yeast. *Proc. Natl. Acad. Sci. USA*. 90:11172–11176.

Fire, A., S. Xu, M.K. Montgomery, S.A. Kostas, S.E. Driver, and C.C. Mello. 1998. Potent and specific genetic interference by double-stranded RNA in *Caenorhabditis elegans*. *Nature.* 391:806–811.

Gaglio, T., M.A. Dionne, and D.A. Compton. 1997. Mitotic spindle poles are organized by structural and motor proteins in addition to centrosomes. *J. Cell Biol.* 138:1055–1066.

Gepner, J., M. Li, S. Ludmann, C. Kortas, K. Boylan, S.J. Iyadurai, M. McGrail, and T.S. Hays. 1996. Cytoplasmic dynein function is essential in *Drosophila melanogaster*. *Genetics.* 142:865–878.

Gönczy, P., and A.A. Hyman. 1996. Cortical domains and the mechanisms of asymmetric cell division. *Trends Cell Biol.* 6:382–387.

Gönczy, P., H. Schnabel, T. Kaletta, A.D. Amores, T. Hyman, and R. Schnabel. 1999. Dissection of cell division processes in the one cell stage *Caenorhabditis elegans* embryo by mutational analysis. *J. Cell Biol.* 144:927–946.

Harada, A., Y. Takei, Y. Kanai, Y. Tanaka, S. Nonaka, and N. Hirokawa. 1998. Golgi vesiculation and lysosome dispersion in cells lacking cytoplasmic dynein. *J. Cell Biol.* 141:51–59.

Hird, S.N., and J.G. White. 1993. Cortical and cytoplasmic flow polarity in early embryonic cells of *Caenorhabditis elegans*. *J. Cell Biol.* 121:1343–1355.

Hirokawa, N., Y. Noda, and Y. Okada. 1998. Kinesin and dynein superfamily proteins in organelle transport and cell division. *Curr. Opin. Cell Biol.* 10: 60–73.

Holzbaur, E.L., and R.B. Vallee. 1994. Dyneins: molecular structure and cellular function. *Annu. Rev. Cell Biol.* 10:339–372.

Hyman, A.A. 1989. Centrosome movement in the early divisions of *Caenorhabditis elegans*: a cortical site determining centrosome position. *J. Cell Biol.* 109:1185–1193.

Hyman, A.A., and J.G. White. 1987. Determination of cell division axes in the early embryogenesis of *Caenorhabditis elegans*. *J. Cell Biol.* 105:2123–2135.

Jan, Y.N., and L.Y. Jan. 1998. Asymmetric cell division. *Nature.* 392:775–778.

Kawasaki, I., Y.H. Shim, J. Kirchner, J. Kaminker, W.B. Wood, and S. Strome. 1998. PGL-1, a predicted RNA-binding component of germ granules, is essential for fertility in *C. elegans*. *Cell.* 94:635–645.

Li, Y.Y., E. Yeh, T. Hays, and K. Bloom. 1993. Disruption of mitotic spindle orientation in a yeast dynein mutant. *Proc. Natl. Acad. Sci. USA*. 90:10096–10100.

Lin, S.X., and C.A. Collins. 1992. Immunolocalization of cytoplasmic dynein to lysosomes in cultured cells. *J. Cell Sci.* 101:125–137.

Lye, R.J., R.K. Wilson, and R.H. Waterston. 1995. Genomic structure of a cytoplasmic dynein heavy chain gene from the nematode *Caenorhabditis elegans*. *Cell Motil. Cytoskeleton.* 32:26–36.

Matthews, L.R., P. Carter, M.D. Thierry, and K. Kemphues. 1998. ZYG-9, a *Caenorhabditis elegans* protein required for microtubule organization and function, is a component of meiotic and mitotic spindle poles. *J. Cell Biol.* 141:1159–1168.

Muhua, L., T.S. Karpova, and J.A. Cooper. 1994. A yeast actin-related protein homologous to that in vertebrate dynactin complex is important for spindle orientation and nuclear migration. *Cell.* 78:669–679.

Murray, A.M. 1991. Cell cycle extracts. *Methods Cell Biol.* 36:591–603.

Nigon, V., P. Guerrier, and H. Monin. 1960. L'architecture polaire de l'oeuf et les mouvements des constituants cellulaires au cours des premières étapes du développement chez quelques nématodes. *Bull. Biol. Fr. Belg.* 93:131–202.

Paschal, B.M., H.S. Shpetner, and R.B. Vallee. 1987. MAP 1C is a microtubule-activated ATPase which translocates microtubules in vitro and has dynein-like properties. *J. Cell Biol.* 105:1273–1282.

Pfarr, C.M., M. Coue, P.M. Grissom, T.S. Hays, M.E. Porter, and J.R. McIn-

tosh. 1990. Cytoplasmic dynein is localized to kinetochores during mitosis. *Nature.* 345:263–265.
Rattner, J.B., and M.W. Berns. 1976. Distribution of microtubules during centriole separation in rat kangaroo (*Potorous*) cells. *Cytobios.* 15:37–43.
Reinsch, S., and E. Karsenti. 1997. Movement of nuclei along microtubules in *Xenopus* egg extracts. *Curr. Biol.* 7:211–214.
Reinsch, S., and P. Gönczy. 1998. Mechanisms of nuclear positioning. *J. Cell Sci.* 111:2283–2295.
Roos, U.P. 1973. Light and electron microscopy of rat kangaroo cells in mitosis. I. Formation and breakdown of the mitotic apparatus. *Chromosoma.* 40:43–82.
Schroer, T.A., J.B. Bingham, and S.R. Gill. 1996. Actin-related protein 1 and cytoplasmic dynein-based motility: what's the connection. *Trends Cell Biol.* 6:212–215.
Shaw, S.L., E. Yeh, P. Maddox, E.D. Salmon, and K. Bloom. 1997. Astral microtubule dynamics in yeast: a microtubule-based searching mechanism for spindle orientation and nuclear migration into the bud. *J. Cell Biol.* 139: 985–994.
Skop, A.R., and J.G. White. 1998. The dynactin complex is required for cleavage plane specification in early *Caenorhabditis elegans* embryos. *Curr. Biol.* 8:1110–1115.
Steuer, E.R., L. Wordeman, T.A. Schroer, and M.P. Sheetz. 1990. Localization of cytoplasmic dynein to mitotic spindles and kinetochores. *Nature.* 345:266–268.
Strome, S., and W.B. Wood. 1983. Generation of asymmetry and segregation of germ-line granules in early *C. elegans* embryos. *Cell.* 35:15–25.
Strome, S., and J. White. 1996. Cleavage plane specification. *Cell.* 84:195–198.
Sulston, J.E., E. Schierenberg, J.G. White, and J.N. Thomson. 1983. The embryonic cell lineage of the nematode *Caenorhabditis elegans. Dev. Biol.* 100: 64–119.
Vaisberg, E.A., M.P. Koonce, and J.R. McIntosh. 1993. Cytoplasmic dynein plays a role in mammalian mitotic spindle formation. *J. Cell Biol.* 123:849–858.
Vallee, R.B., and M.P. Sheetz. 1996. Targeting of motor proteins. *Science.* 271: 1539–1544.
Waddle, J.A., J.A. Cooper, and R.H. Waterston. 1994. Transient localized accumulation of actin in *Caenorhabditis elegans* blastomeres with oriented asymmetric divisions. *Development.* 120:2317–2328.
Waters, J.C., R.W. Cole, and C.L. Rieder. 1993. The force-producing mechanism for centrosome separation during spindle formation in vertebrates is intrinsic to each aster. *J. Cell Biol.* 122:361–372.
Witman, T., H. Boletti, C. Antony, E. Karsenti, and I. Vernos. 1998. Localization of the kinesin-like protein Xklp2 to spindle poles requires a leucine zipper, a microtubule-associated protein, and dynein. *J. Cell Biol.* 143:673–685.